Supplemental Figure Legends

Supplemental Table 1. Patient- and transplant-related variables stratified by preparative regimen for patients who survived 100 days and were relapse-free.

Transplant variable	Numbers and percentages stratified by transplant conditioning		
	Overall (n = 215)	Myeloablative (n = 73)	Non-myeloablative (n = 142)
Sex			
Male	125 (58%)	43 (59%)	82 (58%)
Female	90 (42%)	30 (41%)	60 (42%)
Age at HCT			
Median (range)	51 (1-73)	32 (1-54)	57 (17-73)
Age group			
0-18	16 (7%)	15 (21%)	1 (<1%)
18-45	66 (31%)	45 (62%)	21 (15%)
> 45	133 (62%)	13 (18%)	120 (85%)
Recipient HCMV			
Negative	99 (46%)	36 (49%)	63 (44%)
Positive	116 (54%)	37 (51%)	79 (56%)
Disease group			
ALL	46 (21%)	28 (38%)	18 (13%)
ANLL	88 (41%)	35 (48%)	53 (37%)
CML	5 (2%)	3 (4%)	2 (1%)
Other leukemia	7 (3%)	0 (0%)	7 (5%)
Myelodysplasia	24 (11%)	5 (7%)	19 (13%)
Non-Hodgkin's lymphoma	25 (12%)	2 (3%)	23 (16%)
Hodgkin's lymphoma	15 (7%)	0 (0%)	15 (11%)
Myeloproliferative disease	1 (<1%)	0 (0%)	4 (3%)
Multiple myeloma	4 (2%)	0 (0%)	4 (3%)
Disease risk group			
High	90 (42%)	15 (21%)	75 (53%)
Standard	125 (58%)	58 (79%)	67 (47%)
HCT-comorbidity index			
High	85 (40%)	23 (32%)	62 (44%)
Intermediate	63 (29%)	23 (32%)	40 (28%)
Low	67 (31%)	27 (37%)	40 (28%)
Time from diagnosis to HCT (days) - median (range)	239 (46-5490)	205 (59-3696)	281 (46-5940)

Supplemental Table 2. Patient- and transplant-related variables stratified by preparative regimen for patients who survived 180 days and were relapse-free.

Transplant variable	Numbers and percentages stratified by transplant conditioning			
	Overall (n = 128)	Myeloablative (n = 37)	Non-myeloablative (n = 91)	p-value[1]
Sex				0.68
Male	76 (59%)	23 (62%)	53 (58%)	
Female	52 (41%)	14 (38%)	38 (42%)	
Age at HCT				<0.001
Median (range)	52 (1-73)	34 (1-53)	57 (17-73)	
Age group				<0.001
<18	7 (5%)	6 (16%)	1 (1%)	
18-45	34 (27%)	23 (62%)	11 (12%)	
> 45	87 (68%)	8 (22%)	79 (87%)	
Recipient HCMV				0.56
Negative	64 (50%)	20 (54%)	44 (48%)	
Positive	64 (50%)	17 (46%)	47 (52%)	
Disease group				<0.001
ALL	24 (19%)	13 (35%)	11 (12%)	
ANLL	52 (41%)	19 (51%)	33 (36%)	
CML	3 (2%)	2 (5%)	1 (1%)	
Other leukemia	7 (5%)	0 (0%)	7 (8%)	
Myelodysplasia	13 (10%)	1 (3%)	12 (13%)	
Non-Hodgkin's lymphoma	17 (13%)	2 (5%)	15 (16%)	
Hodgkin's lymphoma	8 (6%)	0 (0%)	8 (9%)	
Myeloproliferative disease	1 (1%)	0 (0%)	1 (1%)	
Multiple myeloma	3 (2%)	0 (0%)	3 (3%)	
Disease risk group				<0.001
High	55 (43%)	4 (11%)	51 (56%)	
Standard	73 (57%)	33 (89%)	40 (44%)	
HCT-comorbidity index				0.21
High	44 (34%)	10 (27%)	34 (37%)	
Intermediate	40 (31%)	10 (27%)	30 (33%)	
Low	44 (34%)	17 (46%)	27 (30%)	
Time from diagnosis to HCT (days) - median (range)	253 (70-3696)	175 (73-3696)	283 (70-3331)	0.09

[1]Fisher's exact test was used for age group, disease group, and risk group, and Chi-square test for the other discrete variables; t-test was used for age and Wilcoxon rank sum test for time from diagnosis to HCT.

Supplemental Table 3. Multivariate regression table corresponding to the clinical association data presented in Figure 8.

Table accompanying Figure 8A

	Hazard Ratio (95% CI)	**p-value**
$CD3^{-}CD56^{dim}CD57^{+}NKG2C^{+}$ NK cells (reference: low/middle tertile)[1]		
High tertile	**0.60 (0.23, 1.60)**	**0.31**
Age (reference: ≥45 yrs)		
<18 yrs	0	>0.99
18-45 yrs	0.23 (0.02, 2.68)	0.23
Disease group (reference: other leukemia)		
ALL	2.37 (0.15, 37.40)	0.54
AML	4.43 (0.37, 52.52)	0.24
CML	0	>0.99
Hodgkin's lymphoma	9.04 (0.37, 218)	0.18
Multiple Myeloma	2.20 (0.13, 36.64)	0.58
Myelodysplasia	0.70 (0.04, 11.30)	0.80
Myeloproliferative Dz	0	>0.99
Non-Hodgkin's Lymphoma	2.40 (0.26, 21.97)	0.44
Disease risk (reference: standard)		
High	1.70 (0.36, 8.09)	0.50
HCT-comorbidity index (reference: low)		
High	1.94 (0.60, 6.26)	0.27
Intermediate	1.65 (0.50, 5.39)	0.41

[1]Low tertile (n=30): < 0.2044 cells/μl, middle tertile (n=30): ≥0.2044 cells/μl, < 0.00242788, high tertile (n=31): ≥ 2.42788 cells/μl.

Supplemental Table 3. Multivariate regression table corresponding to the clinical association data presented in Figure 8.

Table accompanying Figure 8B

	Hazard Ratio (95% CI)	**p-value**
$CD3^{-}CD56^{dim}CD57^{+}EAT\text{-}2^{-}$ NK cells (reference: low/middle tertile)[2]		
High tertile	**0.35 (0.13, 0.99)**	**0.05**
Age (reference: ≥45 yrs)		
<18 yrs	0	>0.99
18-45 yrs	0.34 (0.03, 3.38)	0.36
Disease group (reference: other leukemia)		
ALL	2.87 (0.17, 48.23)	0.46
AML	6.27 (0.52, 75.39)	0.15
CML	0	>0.99
Hodgkin's lymphoma	7.68 (0.36, 165)	0.19
Multiple Myeloma	2.52 (0.15, 41.27)	0.52
Myelodysplasia	0.81 (0.05, 13.22)	0.88
Myeloproliferative Dz	0	>0.99
Non-Hodgkin's Lymphoma	3.11 (0.33, 29.29)	0.32
Disease risk (reference: standard)		
High	1.55 (0.32, 7.38)	0.59
HCT-comorbidity index (reference: low)		
High	2.08 (0.64, 6.79)	0.23
Intermediate	1.86 (0.54, 6.07)	0.33

[2]Low tertile (n=30): < 0.0618165 cells/μl, middle tertile (n=30): ≥ 0.0618165 cells/μl, < 0.00237069, high tertile (n=31): ≥ 2.37069 cells/μl.

Supplemental Table 4. Fluorescently labeled antibodies used for analysis of NK and T cell reconstitution in double cord blood HCT recipients.

Staining panels for NK and T cell phenotypic analysis of transplant samples				
NK cell panel				
Antigen	*Fluorochrome*	*µl/test*	*Vendor*	*Clone*
CD3	BV785	3	Biolegend	OKT3
CD56	PE-Cy7	4	Biolegend	HCD56
CD57	BV605	3	BD Bioscience	NK-1
CD57	FITC	3	Biolegend	HCD57
CD57	APC	3	Biolegend	HCD57
EAT-2 (1°)	N/A	1	ProteinTech	SH2D1B
EAT-2 (2°)	BV421	1	Biolegend	Poly4064
SYK	APC	3	BD Bioscience	4D10.1
FcεRγ	FITC	2	Millipore	2578137
NKG2C	PE	5	R&D Systems	134591
Live/Dead	H7	1:1000	Molecular Probes	N/A
T cell panel				
Antigen	*Fluorochrome*	*µl/test*	*Vendor*	*Clone*
CD3	BV785	3	Biolegend	OKT3
CD56	PE-Cy7	4	Biolegend	HCD56
CD4	PerCP-Cy5.5	3	Biolegend	A161A1
CD8	AF700	3	Biolegend	SK1
CD27	PE	3	Biolegend	M-T271
CD45RA	Pacific Blue	3	Biolegend	HI100
CCR7	APC	3	Biolegend	G043H7
Live/Dead	H7	1:1000	Molecular Probes	N/A
HLA				
Antigen	*Fluorochrome*	*µl/test*	*Vendor*	*Clone*
HLA-B27	FITC	3	Abcam	Ab23840

Supplemental Figure 1

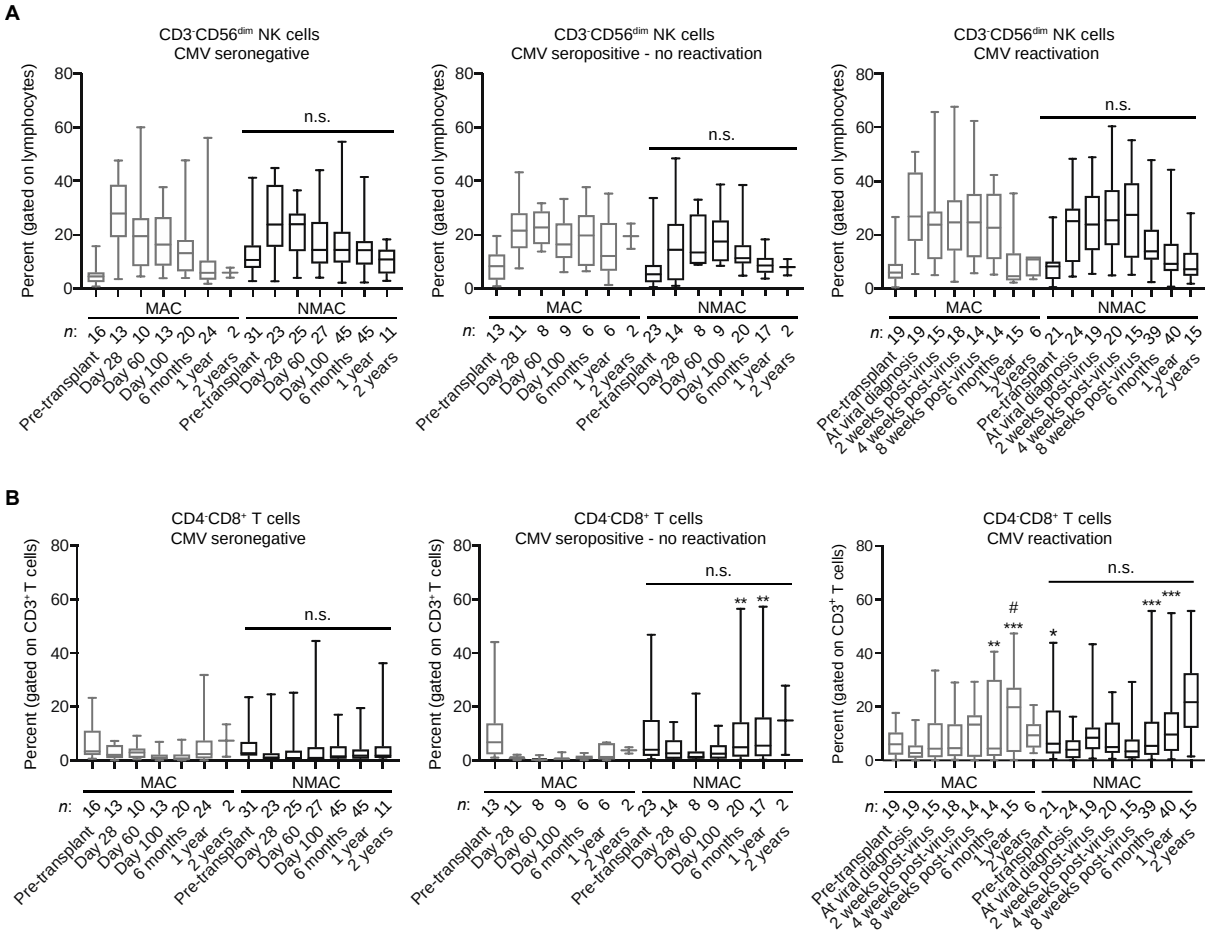

Supplemental Figure 1. Frequencies of total CD3$^-$CD56^{dim} NK cells and CD4$^-$CD8$^+$ T cells are similar between MAC and NMAC transplant recipients. 766 peripheral blood samples drawn from HCT recipients pre- or post-transplant were analyzed by FACS to determine the percentages of (A) CD3$^-$CD56^{dim} NK cells and (B) CD4$^-$CD8$^+$ T cells within the bulk lymphocyte population. The numbers below each bar indicate how many individual transplant samples constitute each group. Solid lines with statistics above the NMAC columns in each graph indicate 2-way ANOVA analyses of the MAC versus NMAC groups. * symbols above individual columns indicate statistically significant differences between average values at those time points compared to matched time points from CMV seronegative HCT recipients calculated using unpaired *t* tests. # symbols above individual columns indicate statistically significant differences between average values at those time points compared to matched time points from HCT recipients that were CMV seropositive without viral reactivation calculated using unpaired *t* tests. *$p <$ 0.05, **$p < 0.01$, ***$p < 0.001$, # $p < 0.05$. Box and whisker plots show means along with minimum and maximum values.

Supplemental Figure 2

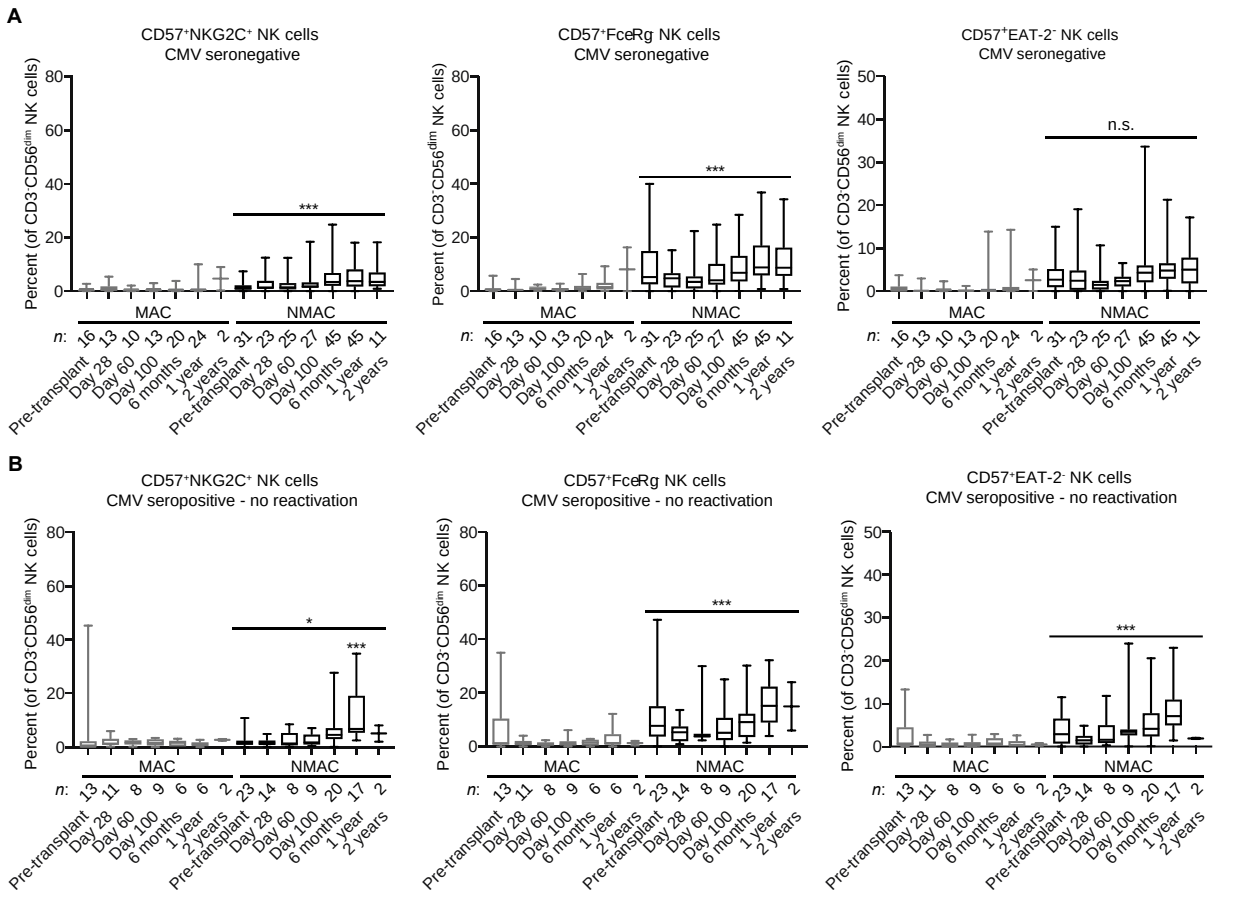

Supplemental Figure 2. Frequencies of adaptive NK cells in HCT recipients that were CMV seronegative or CMV seropositive without viral reactivation. (A) 305 peripheral blood samples drawn from pre- or post-transplant CMV seronegative HCT recipients and (B) 148 peripheral blood samples drawn from CMV seropositive HCT recipients that did not reactivate virus were analyzed by FACS to determine the percentages of $CD57^{+}NKG2C^{+}$, $CD57^{+}Fc\varepsilon R\gamma^{-}$ and $CD57^{+}EAT\text{-}2^{-}$ cells within the $CD3^{-}CD56^{dim}$ NK cell population. The numbers below each bar indicate how many individual transplant samples constitute each group. Solid lines with statistics above the NMAC columns in each graph indicate 2-way ANOVA analyses of the MAC versus NMAC groups. * symbols above individual columns indicate statistically significant differences between average values at those time points compared to matched time points from CMV seronegative HCT recipients calculated using unpaired *t* tests. ***$p <$ 0.001. Box and whisker plots show means along with minimum and maximum values.

Supplemental Figure 3

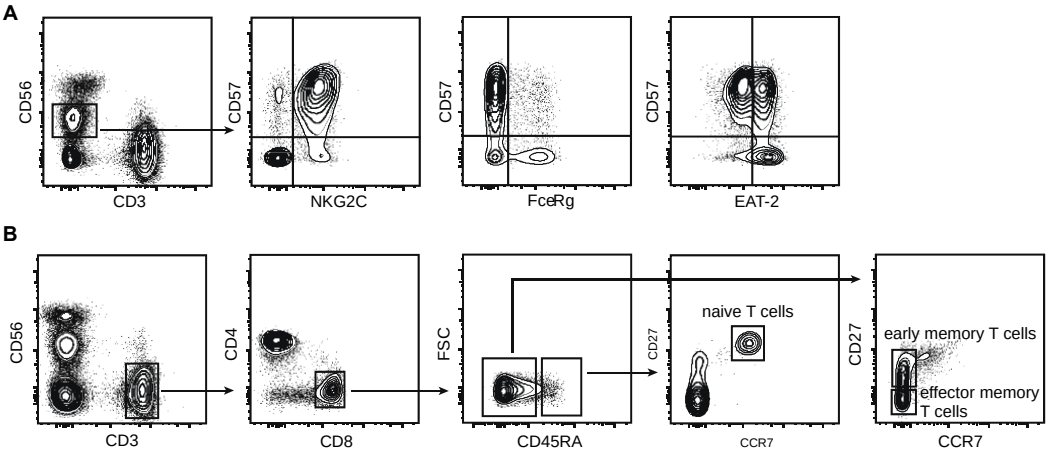

Supplemental Figure 3. Representative FACS plots showing the gating scheme for identifying adaptive NK cell subsets and CD8$^+$ T cell subsets. (A) CD3$^-$CD56^{dim} NK cells were gated and then analyzed further based on expression of CD57 along with NKG2C, EAT-2 or FcεRγ. The adaptive populations were defined as CD57$^+$NKG2C$^+$, CD57$^+$FcεRγ$^-$ and CD57$^+$EAT-2$^-$. (B) CD3$^+$CD56$^-$ T cells were gated first, followed by gating on the CD4$^-$CD8+ population. CD8$^+$ T cells were then gated based on CD45RA expression (CD45RA$^+$ and CD45RA$^-$). CD45RA$^+$ T cells were then gated based on CD27 and CCR7. Naïve CD8$^+$ T cells were defined as CD27$^+$CCR7$^+$. CD45RA$^-$ T cells were also further gated based on CD27 and CCR7. Early memory T cells were defined as CD27$^+$CCR7$^-$, and effector memory T cells were defined as CD27$^-$CCR7$^-$.

Supplemental Figure 4

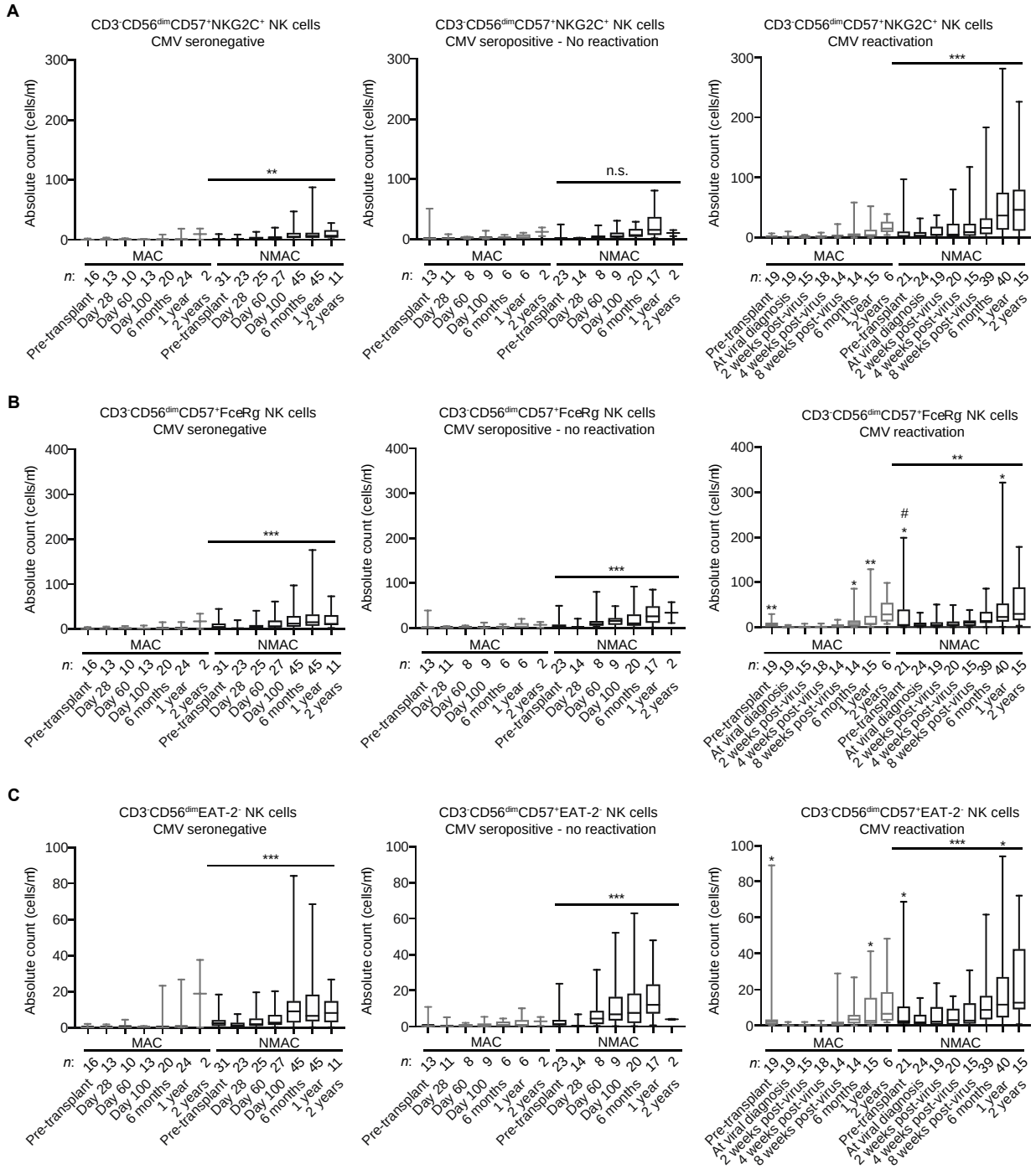

Supplemental Figure 4. Absolute counts for adaptive NK cell subsets during reconstitution from umbilical cord blood progenitors in HCT recipients. 766 peripheral blood samples drawn from HCT recipients pre- or post-transplant were analyzed by FACS and back calculating to absolute lymphocyte counts in order to determine the absolute numbers of $CD57^+NKG2C^+$, $CD57^+Fc\varepsilon R\gamma^-$ and $CD57^+EAT\text{-}2^-$ cells within the $CD3^-CD56^{dim}$ NK cell population. The numbers below each bar indicate how many individual transplant samples constitute each group. Solid lines with statistics above the NMAC columns in each graph indicate 2-way ANOVA analyses of the MAC versus NMAC groups. * symbols above individual columns in the "CMV seropositive – no reactivation" and "CMV reactivation" graphs indicate significant differences between average values at those time points compared to matched time points in the "CMV seronegative" graph calculated using unpaired *t* tests. $*p < 0.05$, $**p < 0.01$, $***p < 0.001$. Box and whisker plots show means along with minimum and maximum values.

Supplemental Figure 5

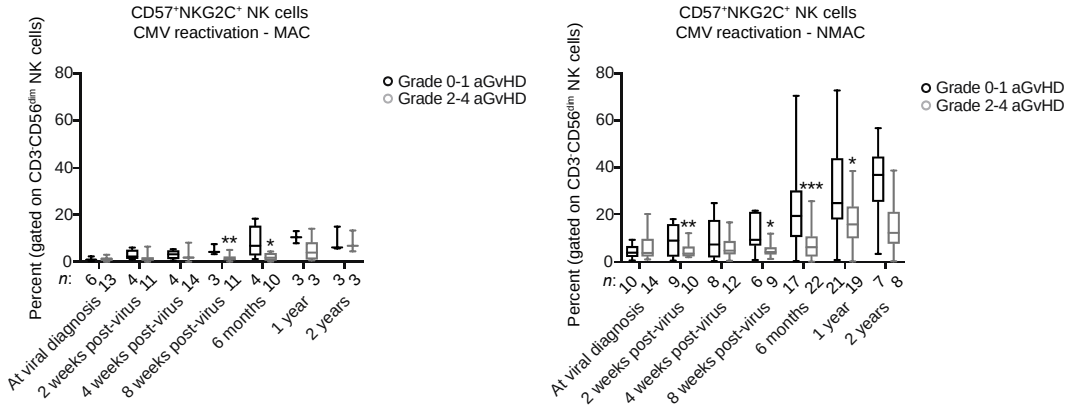

Supplemental Figure 5. Suppressive effect of aGvHD on adaptive NK cell reconstitution in both MAC and NMAC recipients. Peripheral blood samples from MAC (left) and NMAC (right) transplant recipients stratified by aGvHD incidence were analyzed to determine the percentages of adaptive $CD57^{+}NKG2C^{+}$ NK cells at continuous time points post-transplant. Statistical significance was determined using unpaired *t* tests. $*p < 0.05$, $**p < 0.01$, $***p < 0.001$, # $p < 0.05$. Box and whisker plots show means along with minimum and maximum values.

Supplemental Figure 6

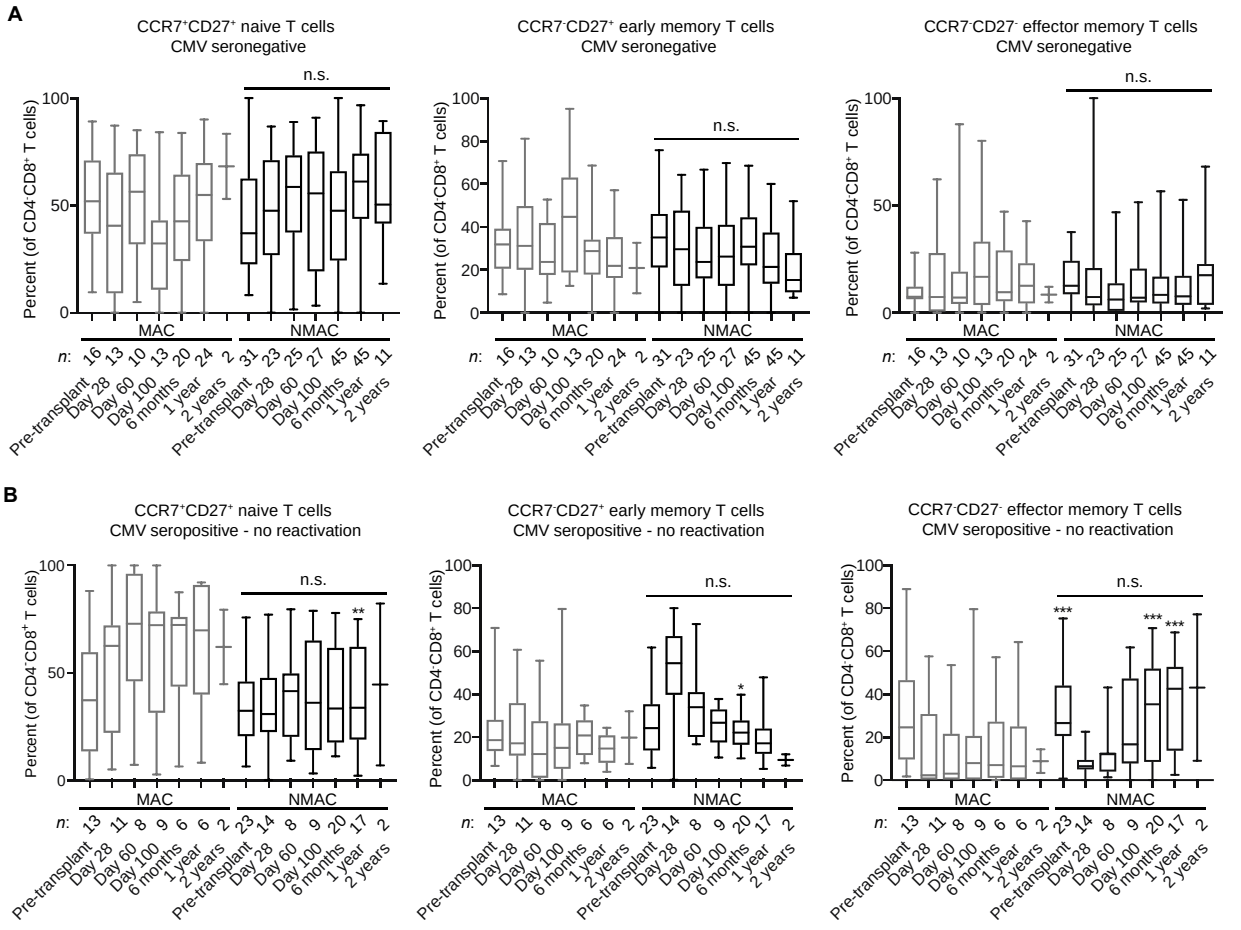

Supplemental Figure 6. Frequencies of CD8$^+$ T cell subsets in HCT recipients that were CMV seronegative or CMV seropositive without viral reactivation. (A) 305 peripheral blood samples drawn from pre- or post-transplant CMV seronegative HCT recipients and (B) 148 peripheral blood samples drawn from CMV seropositive HCT recipients that did not reactivate virus were analyzed by FACS to determine the percentages of naïve, early memory and effector memory cells within the CD3$^+$CD4$^-$CD8$^+$ T cell population. The numbers below each bar indicate how many individual transplant samples constitute each group. Solid lines with statistics above the NMAC columns in each graph indicate 2-way ANOVA analyses of the MAC versus NMAC groups. * symbols above individual columns indicate statistically significant differences between average values at those time points compared to matched time points from CMV seronegative HCT recipients calculated using unpaired *t* tests. *p<0.05, **p<0.01, ***p < 0.001. Box and whisker plots show means along with minimum and maximum values.

Supplemental Figure 7

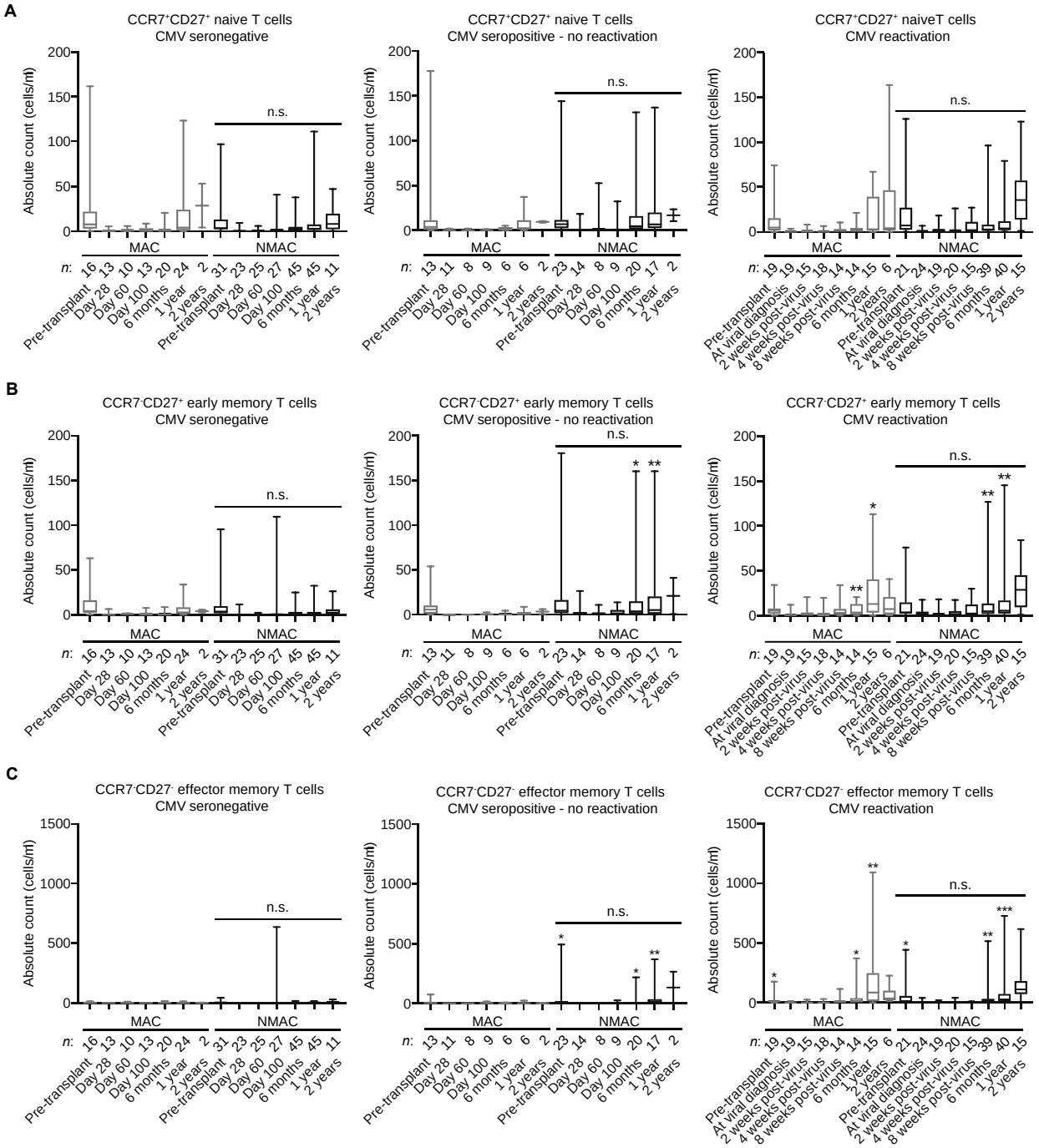

Supplemental Figure 7. Absolute counts for CD8⁺ T cell subsets during reconstitution from umbilical cord blood progenitors in HCT recipients. 766 peripheral blood samples drawn from HCT recipients pre- or post-transplant were analyzed by FACS and back calculating to absolute lymphocyte counts in order to determine the absolute numbers of naïve, early memory and effector memory cells within the $CD3^+CD4^-CD8^+$ T cell population. The numbers below each bar indicate how many individual transplant samples constitute each group. Solid lines with statistics above the NMAC columns in each graph indicate 2-way ANOVA analyses of the MAC versus NMAC groups. * symbols above individual columns in the "CMV seropositive – no reactivation" and "CMV reactivation" graphs indicate significant differences between average values at those time points compared to matched time points in the "CMV seronegative" graph calculated using unpaired *t* tests. *$p < 0.05$, **$p < 0.01$, ***$p < 0.001$. Box and whisker plots show means along with minimum and maximum values.

Supplemental Figure 8

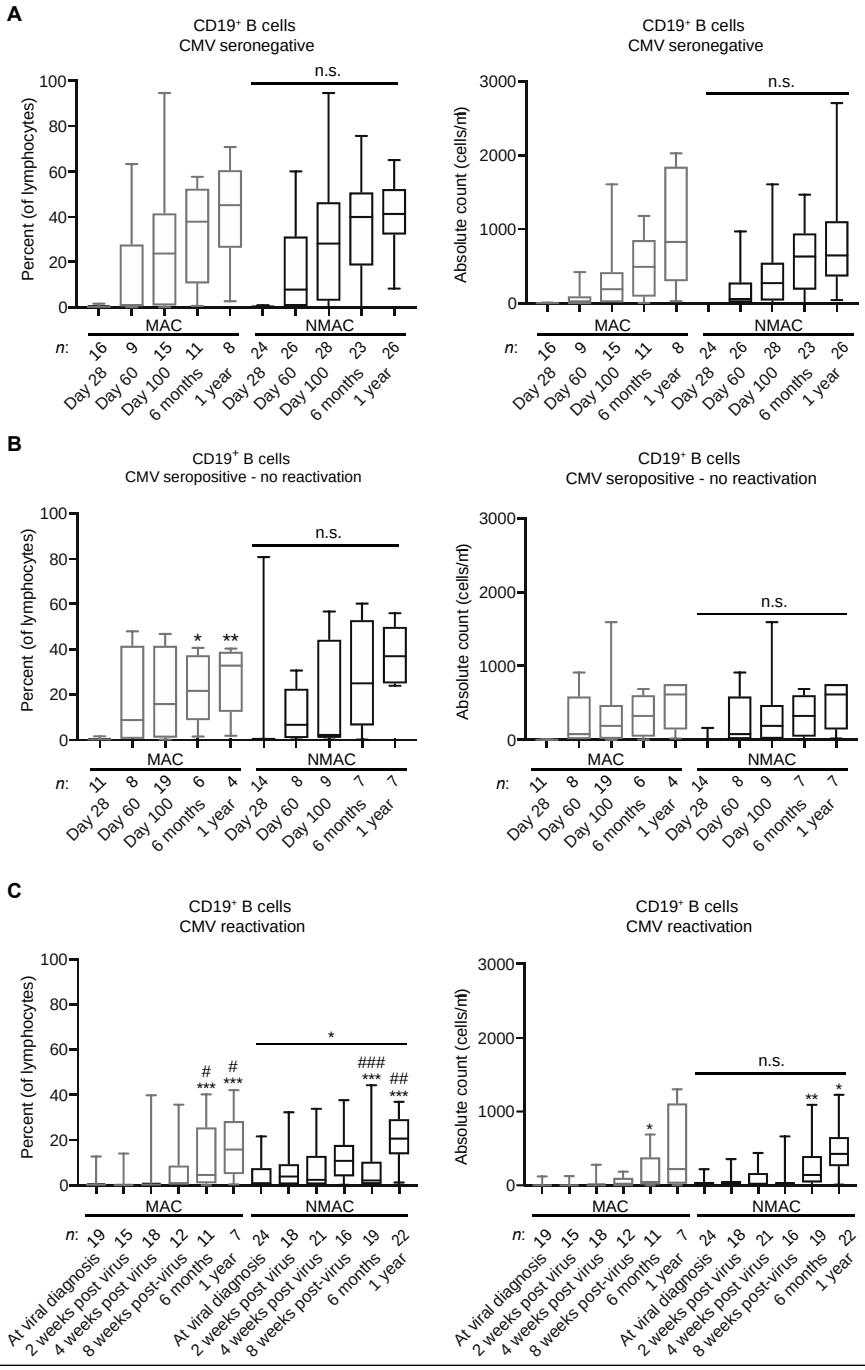

Supplemental Figure 8. CD19$^+$ B cell reconstitution post-HCT stratified by CMV and transplant conditioning. 481 peripheral blood samples drawn from HCT recipients pre- or post-transplant were analyzed by FACS to determine the percentages (left) and the absolute numbers (right) of CD19$^+$ B cells in (A) CMV seronegative recipients, (B) CMV seropositive recipients that did not reactivate virus and (C) CMV seropositive recipients with CMV reactivation. The numbers below each bar indicate how many individual transplant samples constitute each group. Solid lines with statistics above the NMAC columns in each graph indicate 2-way ANOVA analyses of the MAC versus NMAC groups. ***** symbols above individual columns in the "CMV seropositive – no reactivation" and "CMV reactivation" graphs indicate significant differences between average values at those time points compared to matched time points in the "CMV seronegative" graph calculated using unpaired *t* tests. # symbols above individual columns in the "CMV reactivation" graphs indicate significant differences between average values at those time points compared to matched time points in the "CMV seropositive – no reactivation" graph calculated using unpaired *t* tests. *$p < 0.05$, **$p < 0.01$, ***$p < 0.001$, # $p < 0.05$, ## $p < 0.01$, ### $p < 0.001$.

Supplemental Figure 9

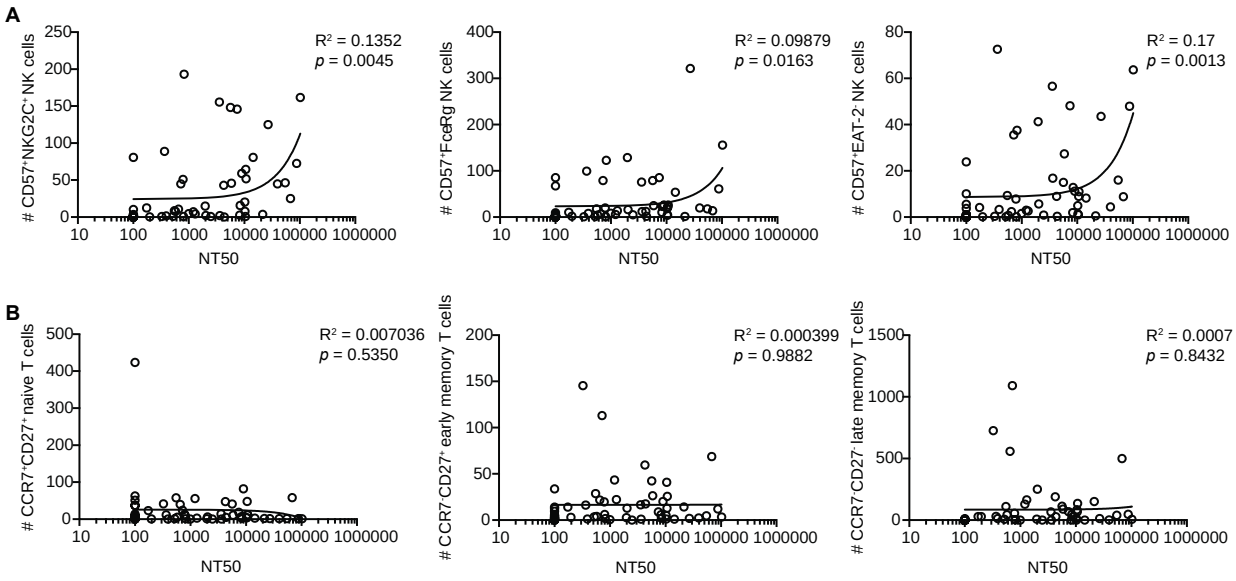

Supplemental Figure 9. Correlations between adaptive NK cell and CD8$^+$ T cell frequencies and CMV neutralizing antibody titers in HCT recipients at 1-year post-transplant. Scatter plots of NT50 values assayed from plasma or serum against matching (A) adaptive NK cell frequencies and (B) CD8$^+$ T cell subset frequencies found in peripheral blood from 58 unique transplant samples from the 1-year post-transplant time point.

Supplemental Figure 10

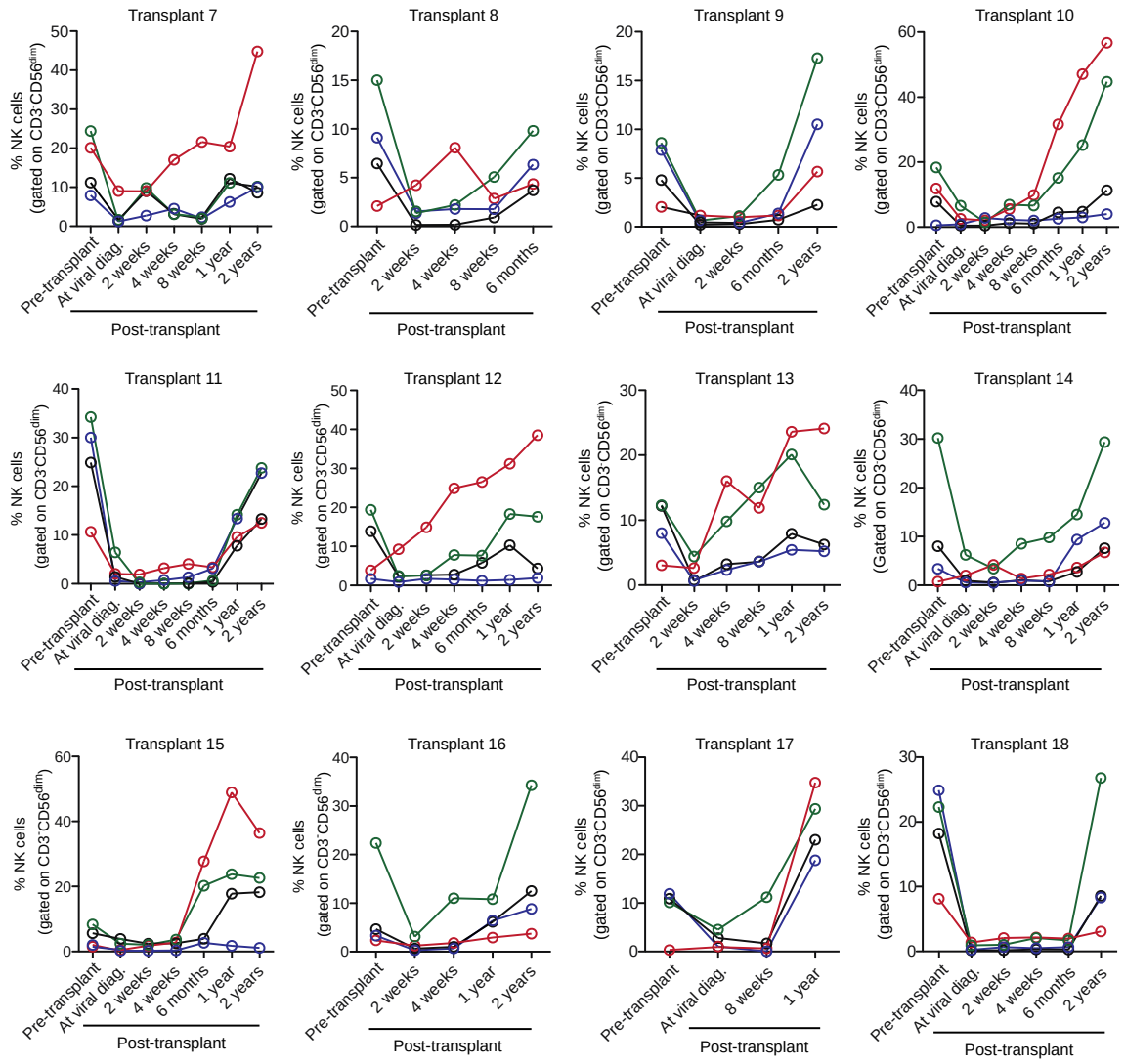

Supplemental Figure 10. Additional graphs showing the frequencies of adaptive NK cell subsets within the recipient CD3$^-$CD56^{dim} NK cell compartment pre-transplant compared to donor-derived NK cells post-transplant. The percentages of adaptive NK cell subsets, defined by expression of CD57 and either NKG2C, FcεRγ, EAT-2 or SYK, in recipient NK cells pre-transplant and donor-derived NK cells at various time points post-transplant were plotted for CMV seropositive NMAC HCT recipients that experienced viral reactivation. All individuals displayed high (> 5%) frequencies of at least one adaptive NK cell subset pre-transplant.

Supplemental Figure 11

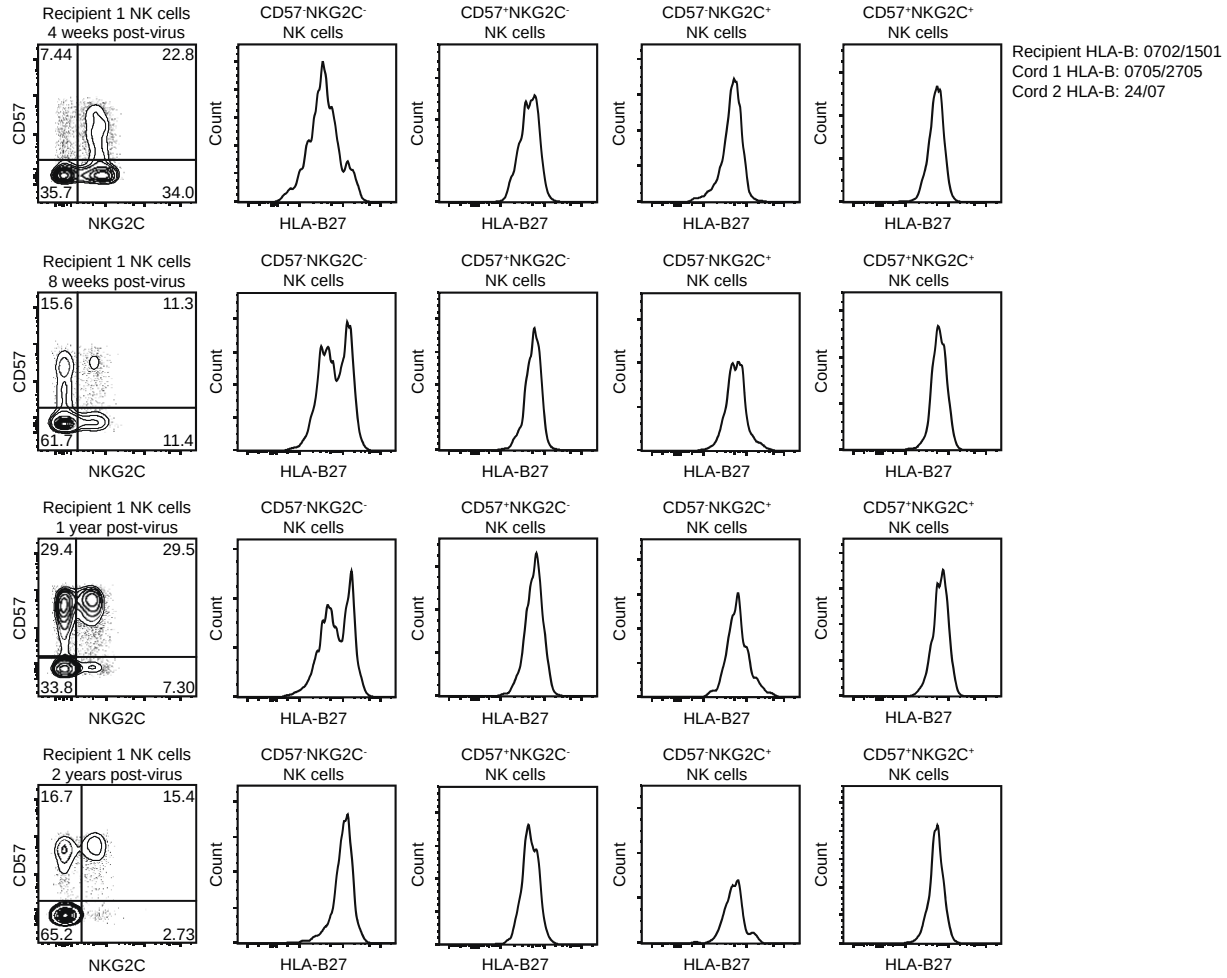

Supplemental Figure 11. Both adaptive and canonical NK cells in recipient blood post-transplant are donor-derived. FACS plots of CD57 and NKG2C expression on gated $CD3^{-}CD56^{dim}$ NK cells from a representative transplant recipient along with HLA-B27 expression on the indicated subsets of NK cells at 4 time points post-transplant. For this transplant the recipient HLA-B genotype was 0702/1501, cord donor 1 was 0702/1501 and cord donor 2 was 24/07.